Variability of surface meteorology and air-sea fluxes observed by R/V *Mirai* during CINDY2011/DYNAMO campaign

Satoru Yokoi (yokoi@jamstec.go.jp), Ayako Seiki, and Takanori Horii
(Japan Agency for Marine–Earth Science and Technology (JAMSTEC), Japan)

1. Introduction and Summary

✓ Introduction & subject of this study

- We examine influence of cumulus convective activity on surface meteorological variables and air-sea heat fluxes observed by R/V *Mirai* during the CINDY2011/DYNAMO campaign.
- Special focus on wind speed changes, and relationship between measures of the influence and convective activity.

✓ Summary

- Since most of the observed convections after October 12 were sporadic and sub-MCS (mesoscale convective systems) scale ones, we can easily identify start and end of the influence.
- We identify 13 cases with only one surface air temperature (T_a) drop, and 9 cases with two T_a drops occurring subsequently.
- Characteristics in T_a, surface humidity (q_a), and wind speed ($|\boldsymbol{u}_s|$) changes are consistent with results in previous studies.
- Anomalies in successive convectively active period are larger than that in primary active period.
- Enhancement of $|\boldsymbol{u}_s|$ tends to terminate quickly compared with T_a and q_a drops.
- Decomposition of $|\boldsymbol{u}_s|$ change into its parallel and rectangular components with respect to $\boldsymbol{u}_s$ in the pre-convective period reveals that the quick termination is due to the parallel component.
- We try to find evidence of convective momentum transport.
- Minimum T_a and difference of maximum $|\boldsymbol{u}_s|$ from $|\boldsymbol{u}_s|$ in the pre-convective period are more representative of the magnitude of the influence than difference of minimum T_a from T_a in the pre-convective period and maximum $|\boldsymbol{u}_s|$ itself.
- We compare variability in the single and double events and that in MCS-scale events in early October.

2. Data

- R/V *Mirai* was deployed at 8°S, 80.5°E
  in Sep. 30 – Oct. 24 and Oct. 30 – Nov. 28 (~52 days)
- Data used:
  - **Surface meteorological observations:**
    Surface wind ($\boldsymbol{u}_s$), temperature (T_a), humidity (q_a), SW, LW, SST
    1-min resolution, with 11-min running mean applied
  - Surface sensible and latent heat fluxes (SHF, LHF) estimated with COARE3.0 bulk flux algorithm (Fairall et al. 1996, 2003).
  - **C-band Doppler radar reflectivity:**
    CAPPI at 2km height, 1-km horizontal resolution, 10-min intervals.
    R(r km) : Estimated rainfall over a circle with r-km radius.
    Cov(r km) : Fractional area covered with
    radar echo (≥15 dBZ) in a circle with r-km radius.
  - **Radiosonde sounding:** horizontal wind profile ($\boldsymbol{u}$), 3 hourly

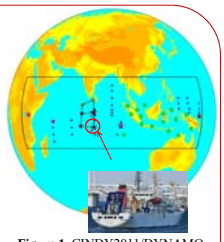

Figure 1. CINDY2011/DYNAMO observation network. The red circle indicate location of R/V *Mirai*.

3. Overall features

- Southeasterly surface wind (~5 m s^{-1}) environment
- Characteristics of convective activity
  - Before Oct. 12: Mesoscale convective system (MCS) events → Composite of 4 MCSs (Section 8).
  - After Oct. 12: Sub-MCS-scale convective systems.

→ It's easy to identify start and end of influence of individual convective systems (Sections 4–7).

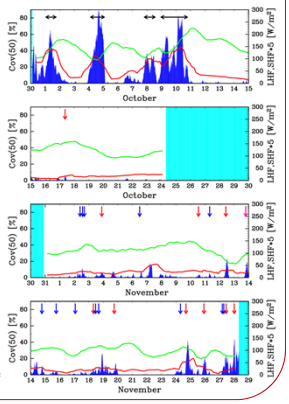

Figure 2. Time series of (red) SHF and (green) LHF, and (blue) Cov(50km). One-day running mean has been applied to SHF and LHF. Note that SHF is quintupled. Black arrows indicate MCS events, and blue (red) arrows indicate single (double) events (see Section 4).

4. Definition of events

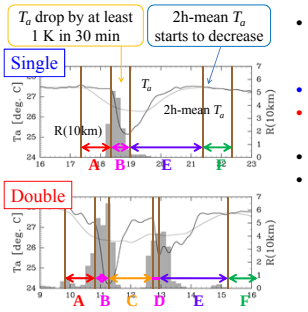

Figure 3. Example of the events.

- We detect sharp T_a drops to identify influence of convective systems.
- **13 single events**: only one drop
- **9 double events**: two drops occurring succeedingly.
- (2 triple events)
- Six Periods:
  - A: pre-convective (1hr)
  - B: (primary) convectively active
  - C: inter-convective
  - D: successive convectively active
  - E: recovery
  - F: post-recovery (1hr)

5. Composite analysis

- Sharp drops of T_a and q_a, and enhancement of $|\boldsymbol{u}_s|$.
- T_a and q_a are recovered gradually, while the enhancement of $|\boldsymbol{u}_s|$ terminates quickly.
- Resultantly, SHF and LHF increase during the active period.
- Note that anomalies are generally greater in successive active period than in primary active period of the double events.

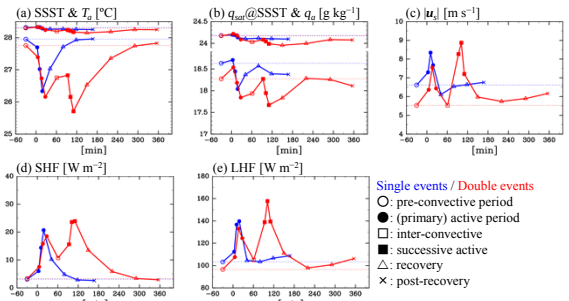

Figure 4. Composite for single (blue) and double (red) events. (a) Skin sea surface temperature (SSST) and T_a, (b) saturated specific humidity at SSST and q_a, (c) $|\boldsymbol{u}_s|$, (d) SHF, and (e) LHF.

6. Surface wind change

- Surface wind change ($\boldsymbol{u}_s' \equiv \boldsymbol{u}_s - \boldsymbol{u}_{s0}$; $\boldsymbol{u}_{s0}$ is $\boldsymbol{u}_s$ in the pre-convective period) can be decomposed into its parallel and rectangular component w.r.t. $\boldsymbol{u}_{s0}$:

$$u_{s//} \equiv (\boldsymbol{u}_s' \cdot \boldsymbol{u}_{s0})/|\boldsymbol{u}_{s0}|, \quad u_{s\perp} \equiv \boldsymbol{u}_s' - u_{s//}\,\boldsymbol{u}_{s0}/|\boldsymbol{u}_{s0}|.$$

- The termination of the enhancement of $|\boldsymbol{u}_s|$ is primarily caused by $u_{s//}$, which is negative in the inter-convective and recovery periods (Fig. 5).
- Note that the centroid of radar echo indicates that ensemble of convective systems move northwestward, almost parallel to $\boldsymbol{u}_0$ (Fig. 6).

Discussion on convective momentum transport

- $u_{//}$ ($\equiv \{(\boldsymbol{u} - \boldsymbol{u}_s) \cdot \boldsymbol{u}_s\}/|\boldsymbol{u}_s|$) is negative in the middle troposphere (Fig. 7).
- Since convection tends to mix the momentum vertically, $u_{s//}$ averaged over the course of the events is expected to be negative.
- However, the averaged $u_{s//}$ is negative for only 13 out of 22 events (slightly more than the half (11)) (Fig. 8).
  - Note that we should consider how $u_{s//}$ becomes negative.

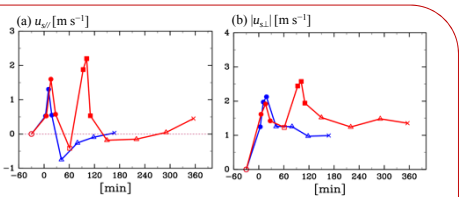

Figure 5. The same as Fig. 4, except for (a) $u_{s//}$ and (b) $|u_{s\perp}|$.

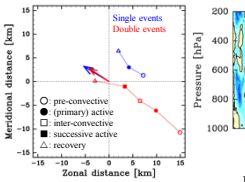

Figure 6. Composite location of the centroid of radar echo in each period, with vectors indicating $\boldsymbol{u}_{s0}$.

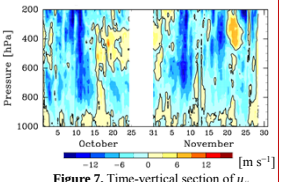

Figure 7. Time-vertical section of $u_{//}$.

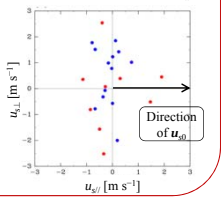

Figure 8. Scatter plot of ($u_{s//}$, $u_{s\perp}$) averaged over the course of individual events (convectively active, inter-convective, and recovery periods). Blue (red) dots indicate single (double) events.

7. Individual active periods

- R(10 km) and Cov(10 km) is positive (>0) for most of the active periods.
- Two measures of the influence of convective activity (minimum T_a ($T_{a\mathrm{Min}}$), maximum $|\boldsymbol{u}_s|$ ($|\boldsymbol{u}_s|_{\mathrm{Max}}$)) and measures of convective activity (R(r km) and Cov(r km)) are compared.
- $T_{a\mathrm{Min}}$ and $|\boldsymbol{u}_s|_{\mathrm{Max}} - |\boldsymbol{u}_{s0}|$ seems to be more representative of the influence than $T_{a\mathrm{Min}} - T_{a0}$ (T_{a0}: T_a in the pre-convective period) and $|\boldsymbol{u}_s|_{\mathrm{Max}}$.
- The measures of the influence are tightly related to radar signals only near the observation point (within 10 km distance).

Table 1. Correlation coefficients between T_a and $|\boldsymbol{u}_s|$ measures and Cov(10km). Asterisks indicate 99.9% significance.

	Cov(10km)		$-T_{a\mathrm{Min}}$	$T_{a0} - T_{a\mathrm{Min}}$
$-T_{a\mathrm{Min}}$	+0.57*	$\lvert\boldsymbol{u}_s\rvert_{\mathrm{Max}}$	+0.31	+0.42*
$T_{a0} - T_{a\mathrm{Min}}$	+0.22	$\lvert\boldsymbol{u}_s\rvert_{\mathrm{Max}} - \lvert\boldsymbol{u}_{s0}\rvert$	+0.68*	+0.40*
$\lvert\boldsymbol{u}_s\rvert_{\mathrm{Max}}$	+0.23			
$\lvert\boldsymbol{u}_s\rvert_{\mathrm{Max}} - \lvert\boldsymbol{u}_{s0}\rvert$	+0.47*			

N = 37 convectively active periods
(13 single + 2 × 9 double + 3 × 2 triple events)

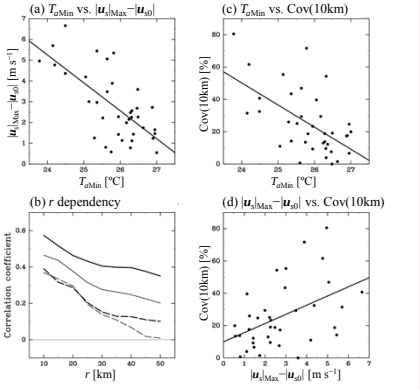

Figure 9. (a) Scatter plot of $T_{a\mathrm{Min}}$ versus $|\boldsymbol{u}_s|_{\mathrm{Max}} - |\boldsymbol{u}_{s0}|$ for individual active periods. (b) Correlation coefficients of radar-estimated variables [Cov(r km) (solid) and R(r km) (broken)] with $-T_{a\mathrm{Min}}$ (thick) and $|\boldsymbol{u}_s|_{\mathrm{Max}} - |\boldsymbol{u}_{s0}|$ (thin). Horizontal axis represents r [km]. (c) The same as in (a), except for $T_{a\mathrm{Min}}$ versus Cov(10km). (d) The same as in (a), except for $|\boldsymbol{u}_s|_{\mathrm{Max}} - |\boldsymbol{u}_{s0}|$ versus Cov(10km).

8. Composite of the four MCSs

- In contrast to the single and double events, $|\boldsymbol{u}_s|$ continues to increase even after the end of the MCS events, and q_a increases during the events.
- As a result, LHF continues to increase even after the end of the MCS, which is completely different from Fig. 4e.
- Larger overall increases in LHF and SHF compared to the single and double events.

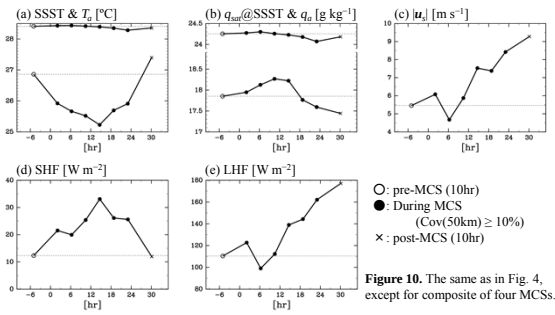

Figure 10. The same as in Fig. 4, except for composite of four MCSs.